MOLECULAR AND CELLULAR BIOLOGY, Aug. 2005, p. 7107–7119 Vol. 25, No. 16
0270-7306/05/$08.00+0 doi:10.1128/MCB.25.16.7107–7119.2005

HANP1/H1T2, a Novel Histone H1-Like Protein Involved in Nuclear Formation and Sperm Fertility

Hiromitsu Tanaka,[1] Naoko Iguchi,[1] Ayako Isotani,[2] Kouichi Kitamura,[1] Yoshiro Toyama,[3] Yasuhiro Matsuoka,[1] Masayoshi Onishi,[1] Kumiko Masai,[1] Mamiko Maekawa,[3] Kiyotaka Toshimori,[3] Masaru Okabe,[2] and Yoshitake Nishimune[1]*

Department of Science for Laboratory Animal Experimentation, Research Institute for Microbial Diseases,[1] Genome Information Research Center,[2] Osaka University, 3-1 Yamadaoka, Suita, Osaka 565-0871, and Department of Anatomy and Developmental Biology, Graduate School of Medicine, Chiba University, Chiba 260-8670,[3] Japan

Received 19 February 2005/Returned for modification 26 April 2005/Accepted 20 May 2005

We cloned a testis-specific cDNA from mice that encodes a histone H1-like, haploid germ cell-specific nuclear protein designated HANP1/H1T2. The HANP1/H1T2 protein was specifically localized to the nuclei of murine spermatids during differentiation steps 5 to 13 but not to the nuclei of mature sperm. HANP1/H1T2 contains an arginine-serine-rich domain and an ATP/GTP binding site, and it binds to DNA, ATP, and protamine. To investigate the physiological role of HANP1/H1T2, we generated *Hanp1*/*H1T2*-disrupted mutant mice. Homozygous *Hanp1*/*H1T2* mutant males were infertile, but females were fertile. Although a substantial number of sperm were recovered from the epididymides, their shape and function were abnormal. During sperm morphogenesis, the formation of nuclei was disturbed and protamine-1 and -2 were only weakly detectable in the nuclei. The chromatin packaging was aberrant, as demonstrated by electron microscopy and biochemical analysis. The mutant sperm exhibited deficient motility and were not competent to fertilize eggs under in vitro fertilization conditions; however, they were capable of fertilizing eggs via intracytoplasmic sperm injection that resulted in the birth of healthy progeny. Thus, we found that HANP1/H1T2 is essential for nuclear formation in functional spermatozoa and is specifically involved in the replacement of histones with protamines during spermiogenesis. At the time of submission of the manuscript, we found an independent publication by Martianov et al. (I. Martianov, S. Brancorsini, R. Catena, A. Gansmuller, N. Kotaja, M. Parvinen, P. Sassone-Corsi, and I. Davidson, Proc. Natl. Acad. Sci. USA 102:2808–2813, 2005) that reported similar results.

The complex process of spermatogenesis includes three major events: proliferation and differentiation of the spermatogonia, meiotic prophase in the spermatocytes, and drastic morphological changes during differentiation from the haploid round spermatids to the mature sperm (24). These events begin after birth, and approximately 35 days are required for the development of mature sperm in the mouse. The differentiation of the haploid germ cells (spermiogenesis) begins at 17 days of age in the mouse. Spermiogenesis involves diverse and complex processes, such as packaging and remodeling of the haploid germ cell nucleus, rearrangement of mitochondria, development of the flagellum, and formation of the acrosome. During this phase, the composition of the chromatin is altered dramatically (29). The changes in the nuclear proteins occur in association with the displacement of general nucleohistones by transition proteins (TNP) and other proteins, including a number of testis-specific histones and nonhistone chromosomal proteins (3, 12, 13, 17, 31) that are subsequently replaced with protamines to form nucleoprotamines (2, 20). The transition from histones to protamines in the chromatin of the haploid germ cells is accompanied by epigenetic changes (19) and the specific formation of nuclei in the sperm (25); these changes are associated with chromosome condensation and the shaping of the nucleus. Recently, mice with null mutations in TNP1 or TNP2 were found to be subfertile (32, 33), and mice with null mutations in both TNP1 and TNP2 were infertile (34). The nuclei of the sperm from the double TNP mutant mice contained protamines, despite the absence of an intermediate nucleosomal state involving TNPs (34).

Thus, the details of the mechanisms of these drastic physiological changes remain to be elucidated. Previously, we isolated cDNA clones of genes that are specifically expressed in mouse haploid germ cells from a subtraction library (9). In this study, we identified and characterized a novel haploid germ cell-specific nuclear protein (HANP1) in the mouse testis that is involved in the histone-protamine transition of sperm chromatin and the subsequent production of functional sperm.

MATERIALS AND METHODS

Cloning of the *Hanp1*/*H1T2* gene. A haploid germ-cell-specific cDNA library was previously generated in the pAP3neo vector by subtracting the mRNA from the testis of a 17-day-old mouse from a cDNA library produced from the testes of an adult (35-day-old) mouse (9). Clones were randomly selected from the subtracted cDNA library and used to probe Northern blots of testis-specific mRNA isolated from mice of various ages. We designated the testis-specific cDNA sequence tags as "transcripts increased in spermiogenesis" (TISP). One of the clones so isolated, TISP-8, possessed an open reading frame encoding a peptide with a high percentage of basic amino acids. Using the TISP-8 partial cDNA as a probe to screen an adult mouse testis library, we isolated the entire cDNA sequence, hereafter designated *Hanp1*/*H1T2*.

Biochemical characterization of HANP1/H1T2. Samples of various tissues were collected from C57BL/6 mice; the germ and somatic cells were prepared

* Corresponding author. Mailing address: Department of Science for Laboratory Animal Experimentation, Research Institute for Microbial Diseases, Osaka University, 3-1 Yamadaoka, Suita, Osaka 565-0871, Japan. Phone: 81-6-6879-8335. Fax: 81-6-6879-8339. E-mail: nishimun@biken.osaka-u.ac.jp.

from the testes as described in our previous report (16). The total RNAs were extracted from the samples using the RNAzol TM B reagent (Tel-Test Inc., Friendswood, TX) according to the manufacturer's instructions and were quantified by measurement of the optical density.

Synthetic peptides were designed from the deduced amino acid sequence of HANP1/H1T2 (ACH; EVRREISSHHEGKSTRLEKG; residues 71 to 90), synthesized, purified (SAWDY, Kyoto, Japan), and used to produce polyclonal antiserum to HANP1/H1T2 in rabbits.

Samples of various C57BL/6 mouse tissues were lysed with radioimmunoprecipitation assay buffer (10 mM Tris-HCl, pH 7.5; 0.15 M NaCl; 1% NP-40; 0.1% sodium deoxycholate; 0.1% sodium dodecyl sulfate [SDS]; 1 mM EDTA; 1 mM phenylmethylsulfonyl fluoride). Nuclear and cytoplasmic fractions of the testicular germ cells were prepared as described in our previous report (27). After centrifugation, aliquots of the samples (50 μg/lane) were separated by SDS–15% polyacrylamide gel electrophoresis (PAGE), and the proteins were transferred to polyvinylidene difluoride membranes (Millipore, Bedford, MA). The membranes were blocked with TBS-T (25 mM Tris-HCl, pH 7.5; 150 mM NaCl; 50 mM KCl; 0.05% Tween 20) containing 5% nonfat dried milk and then incubated with rabbit anti-HANP1/H1T2 polyclonal antibody diluted 1:1,500 in TBS (25 mM Tris-HCl, pH 7.5; 150 mM NaCl; 50 mM KCl). The membranes were then reacted with horseradish peroxidase-conjugated anti-rabbit immunoglobulin G, and the bound antibodies were detected using a peroxidase staining kit (Wako, Osaka, Japan).

The binding affinity between the HANP1/H1T2 protein and DNA or ATP was determined from the elution profile of HANP1/H1T2, protein from DNA-cellulose columns, or ATP-agarose beads. The nuclear lysate from testicular germ cells was applied to a DNA-cellulose column (Sigma-Aldrich, Tokyo, Japan) with a 0.5-ml bed volume in 50 mM Tris-HCl buffer (pH 7.5). After washing with 50 mM Tris-HCl buffer (pH 7.5), the column was eluted with various concentrations of NaCl, and each fraction was subjected to Western blotting with anti-HANP1/H1T2. To assess the binding affinity of HANP1/H1T2 for ATP, a plasmid encoding an enhanced green fluorescent protein (EGFP)-HANP1/H1T2 fusion protein was transfected into HEK-293 cells. Replicate samples of the transfected and mock-transfected cells were harvested 16 h later and lysed by homogenization in 1 ml of TBS-T buffer. After centrifugation, the cleared lysates were passed through 0.45-μm-pore-size SteraDisk filters (Kurabo, Osaka, Japan). The filtrates were mixed with ATP-agarose beads (Sigma-Aldrich) with a 0.5-ml bed volume in TBS-T buffer. The beads were washed three times with 0.5 ml of TBS-T buffer and eluted by boiling in 100 μl of SDS-PAGE sample buffer. The eluates (30 μl) were subjected to Western blot analysis using anti-GFP rat monoclonal antibodies.

The *Hanp1*/*H1T2*, *Prm1*, *hils1*, and *histone H1c* cDNAs were amplified by PCR and cloned into the EcoRI sites of the pmRFP-C1 and pEGFP-C1 plasmids (Clontech), respectively (13). The resulting clones expressed mRFP-HANP1/H1T2, EGFP-protamine, EGFP-HILS1, mRFP-HILS1, and EGFP-histone H1c fusion proteins and were used for coimmunoprecipitation experiments and for observation of subcellular localization in HEK-293 cells. The HEK-293 cells were transfected with the expression vectors using Lipofectamine Plus reagent (Life Technologies, Inc.).

DNA column chromatography of in vitro-translated HANP1/H1T2, histone H1, and HILS1 was performed to examine the DNA binding ability of each protein. PCR amplification of mouse histone H1 and *hils1* cDNA was performed with a set of synthetic oligonucleotide primers based on the histone H1c and *hils1* sequences (GenBank/EMBL/DDBJ accession numbers NM_015786 and AB022320 [13]). The *Hanp1*/*H1T2* cDNA fragment containing the entire coding region was amplified using PCR with the set of synthetic oligonucleotide primers Hanp1-5′ (5′-GGCCATGGCTGAGGCTGTCCAG-3′), based on the *Hanp1* sequence with a NcoI restriction site, and Hanp1-3′ (5′-GGCCATGGCATTAA GGAGACTCAGTGTCC-3′), also with an NcoI linker. Each PCR product was subcloned into the pET30a expression vector (Novagen) using appropriate restriction enzymes. For in vitro translation using STP2, T7 (Novagen) was used, and both proteins were labeled with ^{35}S-protein labeling mix (Amersham Biosciences), as described by the manufacturer. Aliquots of proteins translated in vitro were applied to double-stranded DNA-cellulose columns (Amersham Biosciences). After sufficient washing with the same buffer as that used for the DNA-binding assay, each column was eluted with five volumes of the same buffer containing seven consecutive concentrations of NaCl (0.1, 0.2, 0.3, 0.5, 1.0, 2.0, and 3.0 M) and denaturing buffer containing 6 M guanidine-HCl and 0.2 M acetic acid. The eluted samples were concentrated by trichloroacetic acid precipitation, and equal fractionation aliquots were subjected to SDS–15% PAGE. The gels were then fixed in a solution of 10% acetic acid with 10% methanol, dried, and autoradiographed using an ImageAnalyzer (Fuji Photo Film).

Construction of the *Hanp1*/*H1T2* targeting vector and production of *Hanp1*/*H1T2* knockout mice. The *Hanp1*/*H1T2*-targeting construct was created by PCR amplification of 5′ and 3′ homology arms of 3.5 and 4.9 kb, respectively, from 129Sv genomic DNA. The oligo primers used for amplification of the homology arms were designed to incorporate synthetic restriction enzyme sites at both ends. The two amplified fragments were digested with the appropriate enzymes and sequentially ligated into the polylinker cloning sites on either side of the neomycin resistance gene in the targeting vector backbone. The targeting vector construct contained the neomycin resistance gene and the thymidine kinase gene, both under the control of the phosphoglycerate kinase promoter. The vector plasmid was linearized by digestion with NotI prior to electroporation into W9.5 embryonic stem (ES) cells. Of the 720 G418-ganciclovir-resistant clones obtained, 4 were found by Southern blot analysis to have undergone the correct homologous recombination. The ES cells from each of the four lines were injected into C57BL/6J blastocysts, resulting in the birth of male chimeric mice. Highly chimeric males were mated with C57BL/6J wild-type females to generate F1 offspring, half of which were heterozygous for the targeted allele. Of the four ES cell lines injected, only one produced a high percentage of germ line chimeras. Heterozygous F_1 males were then crossed to C57BL/6 females to obtain heterozygous F_2 animals. Heterozygous F_2 animals were bred to obtain homozygous mutants and to verify the Mendelian pattern of inheritance. Ten mice older than 3 months of age were used to determine the fertility rate by monitoring three pregnancies in each fertile mouse. The assessment of phenotypic variation and the biochemical analyses were conducted on samples from at least three individuals, as described below.

Morphological assessment of testis and epididymal sperm. For immunohistochemical observation of HANP1/H1T2 expression, testes were collected from knockout and control mice, fixed in Carnoy's fixative, embedded in paraffin, and sectioned at a thickness of 8 μm. Sperm from the cauda epididymis were harvested, dried on glass slides, and fixed in Carnoy's fixative for 10 min. The samples were treated with 0.05 M β-mercaptoethanol in TBS before incubation with the appropriate monoclonal antibodies, as previously described (26, 34). For electron microscopic observations, the animals were perfused with 3% glutaraldehyde in HEPES buffer (10 mM HEPES, 145 mM NaCl). After fixation with 1% osmium tetroxide, the testes and cauda epididymides were embedded in Epon resin. Selected areas were sectioned and examined.

Analysis of sperm. The germ cell fractions were prepared from the testes as described in our previous report (16). The nuclei of germ cells and sperm were prepared by sonication, and the basic proteins were extracted and separated by PAGE on acid-urea gels (33). The fractions from three mice were loaded in duplicate on each of two acid-urea gels. One gel was stained with Coomassie brilliant blue to identify the nuclear proteins, and the other was used for Western blot analysis.

Fluorescence-activated cell sorting (FACS) analysis was performed to determine the extent of DNA condensation in sperm from the *Hanp1*/*H1T2* mutant mice, as previously described (33). Sperm were isolated from the cauda epididymides of mutant and control mice. After incubation for 1 h in TYH medium (30), the sperm were subjected to mild sonication and azide was added to a final concentration of 0.025%. The sperm were then stained with propidium iodide and analyzed on a flow cytometer.

Computer-assisted sperm analysis was performed to examine sperm motility, as previously described (28). At least 200 sperm were counted in order to evaluate the percentage of progressively motile sperm, the straight-line velocity, the curvilinear velocity (VCL), the amplitude of lateral head displacement, and linearity. Only the VCL data were reported.

In vitro fertilization assays were performed as previously described (30). Briefly, sperm samples were collected from the cauda epididymides of each male, capacitated in TYH medium at 37°C for 1 h, and then introduced into oocytes with cumulus cells. The inseminated oocytes were placed in 0.3 ml of TYH droplets, covered with mineral oil, and incubated at 37°C in 5% CO_2. After 24 h, successfully fertilized eggs were counted and transplanted into the uteri of pseudopregnant females.

Intracytoplasmic sperm injection (ICSI) was performed as described by others (15). Briefly, sperm collected from the epididymides were suspended in 12% polyvinylpyrolidone (360 kDa) and decapitated with one Piezo pulse (Prime Tech, Tokyo, Japan). The detached heads were introduced into the cytoplasm of unfertilized cumulus-free eggs. After incubation in kSOM medium for 24 h (11), the eggs, at the two-cell stage, were implanted into pseudopregnant females.

RESULTS

The testis-specific *Hanp1*/*H1T2* gene encodes a histone H1-like protein. To provide molecular tools for the examination of the processes involved in sperm morphogenesis, we had pre-

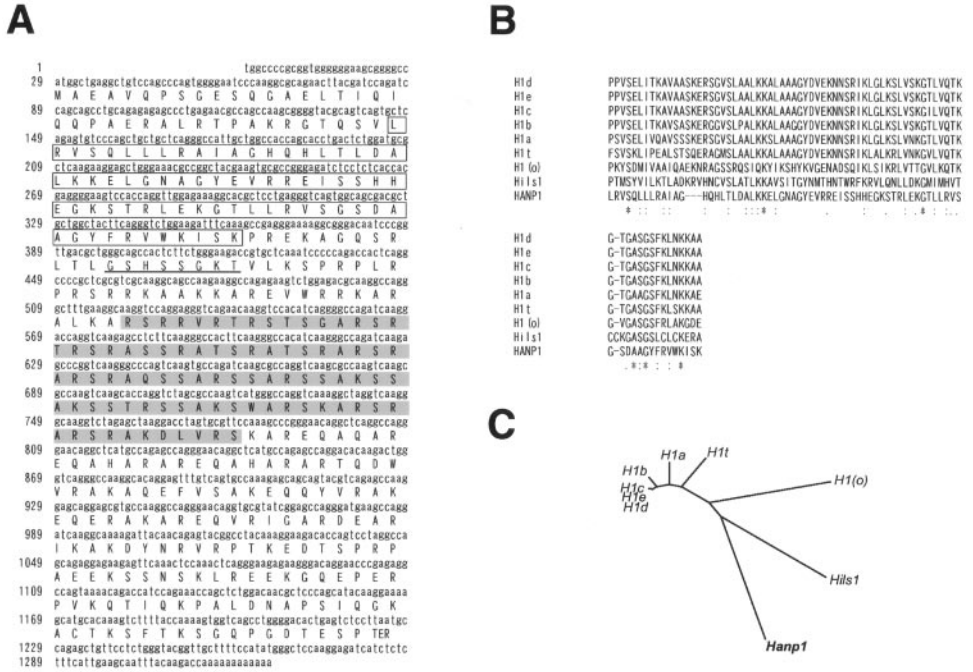

FIG. 1. Sequence analyses of the *Hanp1/H1T2* gene. (A) The full-length sequence of the *Hanp1/H1T2* cDNA (DNA Data Base of Japan, accession numbers AB016273 and AY496853). The box, bar, and shadowed box indicate the putative histone globular domain, ATP-binding site, and RS domain, respectively. (B) The alignment of the deduced amino acid sequence of the globular domain of HANP1/H1T2 with various histone H1 protein sequences. The asterisks and dots indicate similar and homologous amino acids, respectively. (C) A phylogenetic tree of the globular domains of various histone H1 proteins generated using the neighbor-joining method.

viously isolated many cDNA clones that are specifically expressed in testicular germ cells from a subtracted cDNA library produced using haploid germ cell-specific cDNA clones (9). In this study, we found that one clone, designated TISP-8 for transcript increased in spermiogenesis (TISP), encoded a protein containing an extensive series of basic amino acids. Using the TISP-8 partial cDNA as a probe, we isolated a complete cDNA clone, subsequently designated *Hanp1/H1T2*, from an

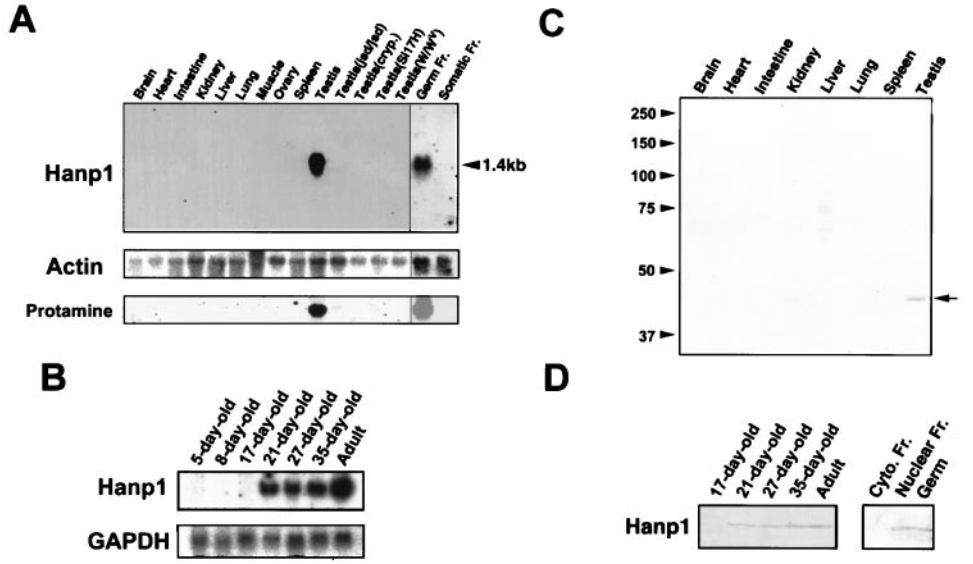

FIG. 2. The expression profiles of *Hanp1/H1T2* mRNA (A and B) and protein (C and D) in mouse tissues. (A) Total RNA was prepared from various organs and hybridized with a *Hanp1/H1T2*-specific probe. Cells recovered from adult mouse testes were separated into germ and somatic cell fractions. (B) The expression of *Hanp1/H1T2* mRNA in the testes at different stages of development (numbers indicate days of age). Western blot analysis of HANP1/H1T2 expression using anti-HANP1/H1T2 rabbit antiserum in various adult mouse tissues (C) and in the testes at different stages of development and in subcellular fractions of testicular germ cells (D). The cryptorchid (cryp.) testes and mutant testes of *jsd/jsd W/Wv S117H/S117H* mice do not have spermatocytes and more differentiated germ cells after 12 weeks of age. Fr., fraction.

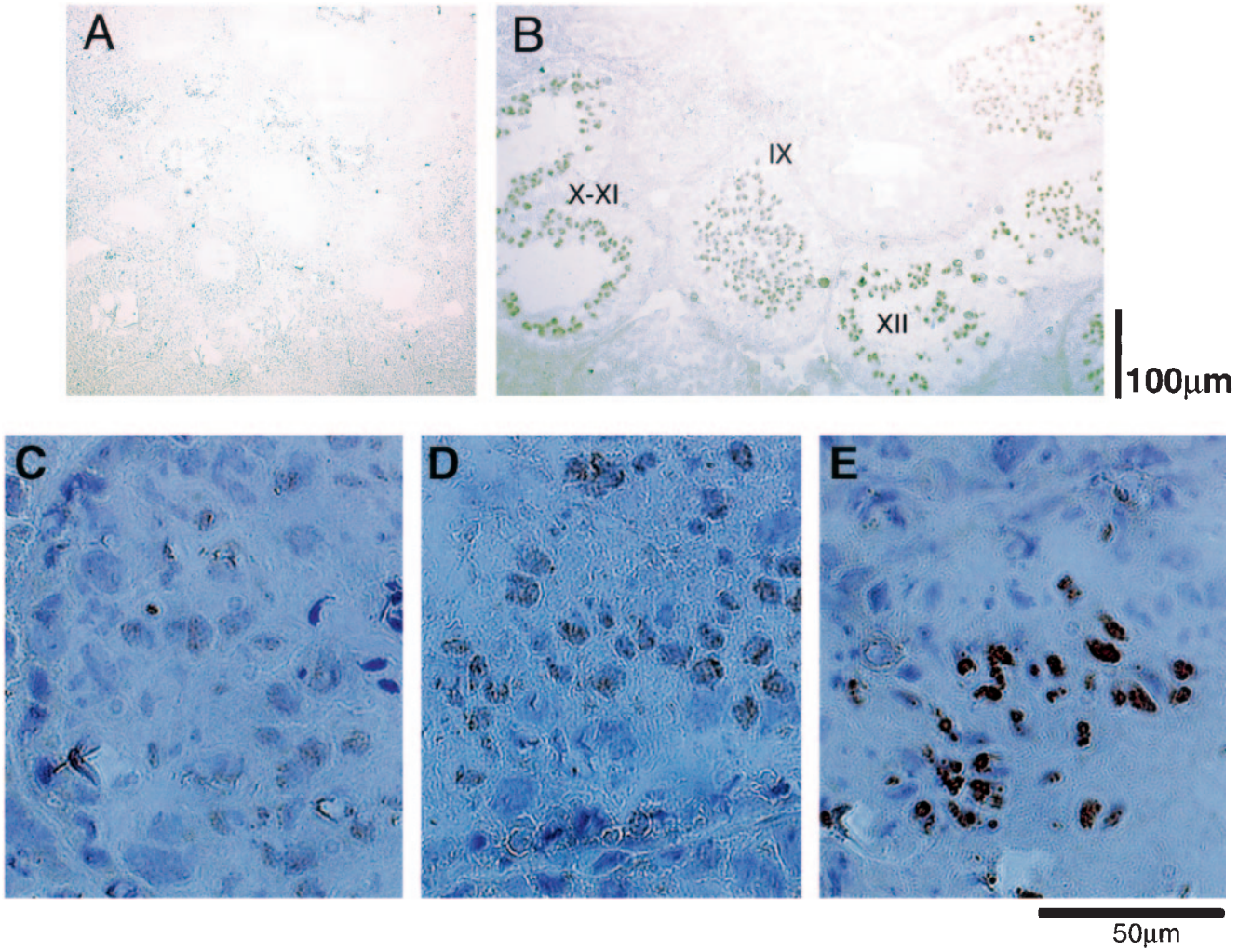

FIG. 3. Expression of HANP1/H1T2 in cross sections of the mouse testis. Immunohistochemical staining of testis tissue sections with preimmune serum (A) or anti-HANP1/H1T2 rabbit serum (B to E). Expression of HANP1/H1T2 during developmental stages V and VI (C), IX (D), and X and XI (E) of the seminiferous tubules. Higher magnification images of each stage were counterstained with hematoxylin (blue). The nuclei of round and elongated spermatids were strongly stained with anti-HANP1/H1T2 antibody (brown).

adult mouse testis library. The complete *Hanp1*/*H1T2* nucleotide sequence (DNA Data Bank of Japan, accession number AB016273), and the deduced amino acid sequence are shown in Fig. 1. The deduced amino acid sequence of the HANP1/H1T2 protein consisted of a region homologous to histone H1, an ATP/GTP-binding site motif A, an RS domain consisting of arginine-serine repeats, and 14 phosphorylation sites for protein kinase C (consensus sequence, S/T-X-R/K). The basic amino acids lysine and arginine composed 25% of the total amino acids predicted from the *Hanp1*/*H1T2* cDNA sequence (Fig. 1). Phylogenetic analysis of HANP1/H1T2 and the globular domains of histone H1 showed that HANP1/H1T2 probably shares a common ancestor with various histone H1s (Fig. 1C) and that it is conserved in the human (data not shown).

***Hanp1*/*H1T2* is specifically expressed in haploid germ cells.** Tissue-specific Northern blot analysis had previously shown that *Hanp1*/*H1T2* mRNA was exclusively expressed as a 1.4-kb transcript in the adult mouse testis but not in the testes of younger animals, in cryptorchid mice, or in mutants having no differentiated germ cells (7). In testicular cells, the expression of *Hanp1*/*H1T2* mRNA was not detected in somatic cells and was limited to germ cells (Fig. 2A) in animals older than 21 days of age (Fig. 2B), indicating that the positive cells were likely to be spermatids. Western blot analysis using anti-HANP1/H1T2 antiserum detected a 44-kDa band in the testes of mice older than 21 days (Fig. 2D) but showed no positive bands in sperm (data not shown). The HANP1/H1T2 protein was exclusively detected in the nuclear fraction (Fig. 2C and D) in Western blot analysis of subcellular extracts from testicular germ cells.

***Hanp1*/*H1T2* expression is localized to the nucleus.** The development of mouse haploid spermatids has been classified into 16 sequential steps following meiotic division (24). The immunohistochemical examination of the adult mouse testis showed that the nuclei of spermatids in developmental steps 5 to 13 were positive for HANP1/H1T2 (Fig. 3), which was consistent with the findings from the Western blots of adolescent testes and subcellular germ cell fractions (Fig. 2D). These

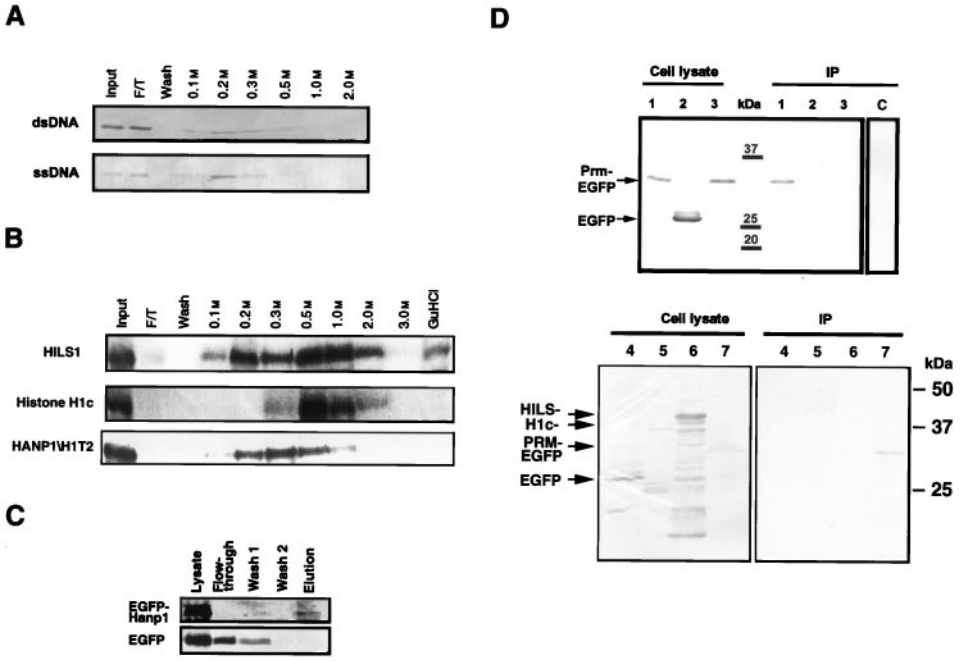

FIG. 4. Biochemical characterization of HANP1/H1T2 protein. (A) DNA binding assay with double-stranded (ds) or single-stranded (ss) DNA-cellulose columns. The chromatography conditions are indicated at the top. Input, the amount of HANP1/H1T2 applied to each column; F/T, flowthrough; Wash, wash fraction; numbers indicate the concentrations of NaCl in the elution buffer. The total protein contained in each fraction was electrophoresed, and Western blots were performed using anti-HANP1/H1T2 antiserum. (B) In vitro-translated and ^{35}S-labeled HANP1/H1T2, Hils1, or histone H1c protein was applied to a double-stranded DNA cellulose minicolumn and eluted with increasing concentrations of NaCl. Aliquots (wash and 0.1 to 3.0 M NaCl were 1/4 volume; the GuHCl was 1/12 volume) of each fraction were separated by SDS-PAGE, and the gels were autoradiographed. F/T and GuHCl represent the flowthrough fraction and denaturing buffer, respectively (13). (C) ATP binding assay on ATP-Sepharose columns. EGFP or EGFP-HANP1/H1T2 recombinant protein was applied to ATP-Sepharose affinity columns and washed with TBS-T buffer (wash fractions 1 and 2). The ATP-Sepharose was eluted by boiling in SDS-PAGE sample buffer, and Western blots were performed using anti-EGFP rat monoclonal antibody. (D) Coimmunoprecipitation of recombinant proteins mRFP-HANP1/H1T2 EGFP–protamine-1, EGFP-histone H1, and EGFP-HILS1. Recombinant proteins were coexpressed in HEK293 cells and electrophoresed (cell lysate) or coimmunoprecipitated with anti-mRFP rabbit serum and protein A-Sepharose beads (IP). Lane 1, EGFP–protamine-1 and mRFP-HANP1/H1T2; lanes 2 and 4, EGFP control and mRFP-HANP1/H1T2; lanes 3 and 7, EGFP–protamine-1 and mRFP control; lane 5, EGFP-histone H1 and mRFP-HANP1/H1T2; lane 6, EGFP-HILS1 and mRFP-HANP1/H1T2; lane C, EGFP–protamine-1 and mRFP-HILS1. Western blots were conducted using anti-EGFP rat monoclonal antibody. Numbers in the center of the panel indicate molecular mass markers (kilodaltons).

results indicated that the HANP1/H1T2 protein is localized to the spermatid nuclei and that the timing of *Hanp1*/*H1T2* gene transcription and translation is precisely regulated during the development of male germ cells.

HANP1/H1T2 is able to directly or indirectly bind to DNA, ATP, and protamines. The nuclear localization and elevated basic amino acid content of HANP1/H1T2 suggested an association of HANP1/H1T2 protein with nucleic acids. To examine the DNA binding activity of endogenous HANP1/H1T2 protein in male germ cells, testicular extracts were applied to double- or single-stranded calf thymus DNA-cellulose minicolumns, and the proteins were eluted with stepwise increasing concentrations of NaCl. HANP1/H1T2 was detected mainly in the fractions eluted from both types of DNA columns with 0.1 to 0.3 M NaCl (Fig. 4A), indicating that HANP1/H1T2 or its complexes bind to both double- and single-stranded DNA.

HANP1/H1T2 was also detected in the flowthrough fraction. The reapplication of the flowthrough fraction to fresh DNA-cellulose minicolumns showed the HANP1/H1T2 present in the flowthrough fraction rarely binds to the DNA columns (data not shown). Next, we compared the DNA binding ability with other linker histones expressed in spermiogenesis. HANP1 ability is weaker than both histone H1 and *hils1* (Fig. 4B). These results indicated that HANP1/H1T2 or its complexes might have alternative forms that are unable to bind to DNA. HANP1/H1T2 protein was also found to bind to ATP-agarose minicolumns, suggesting that ATP might act as a cofactor in the regulation of HANP1/H1T2 (Fig. 4C). We also examined the ATPase activity of mRFP-HANP1/H1T2 recombinant protein. However, we did not detect activity in the immunoprecipitant of an extract of HEK 293 cells expressing mRFP-HANP1/H1T2 (data not shown). HANP1/H1T2 was identified for the first time as a histone H1-like protein having an RS domain that is transiently expressed during mouse spermiogenesis.

Members of the SR protein family having RS domains play important roles in the tissue-specific regulation of alternative pre-mRNA splicing (10). Recently, it was also reported that RS domains were involved in protein-protein interactions (22). As HANP1/H1T2 is expressed in nuclei at the time of the transition from histones to protamines in chromatin during spermiogenesis, we examined whether HANP1/H1T2 associates with protamine-1 by using ectopic expression of tagged proteins, because neither the anti-HANP1/H1T2 nor anti-pro-

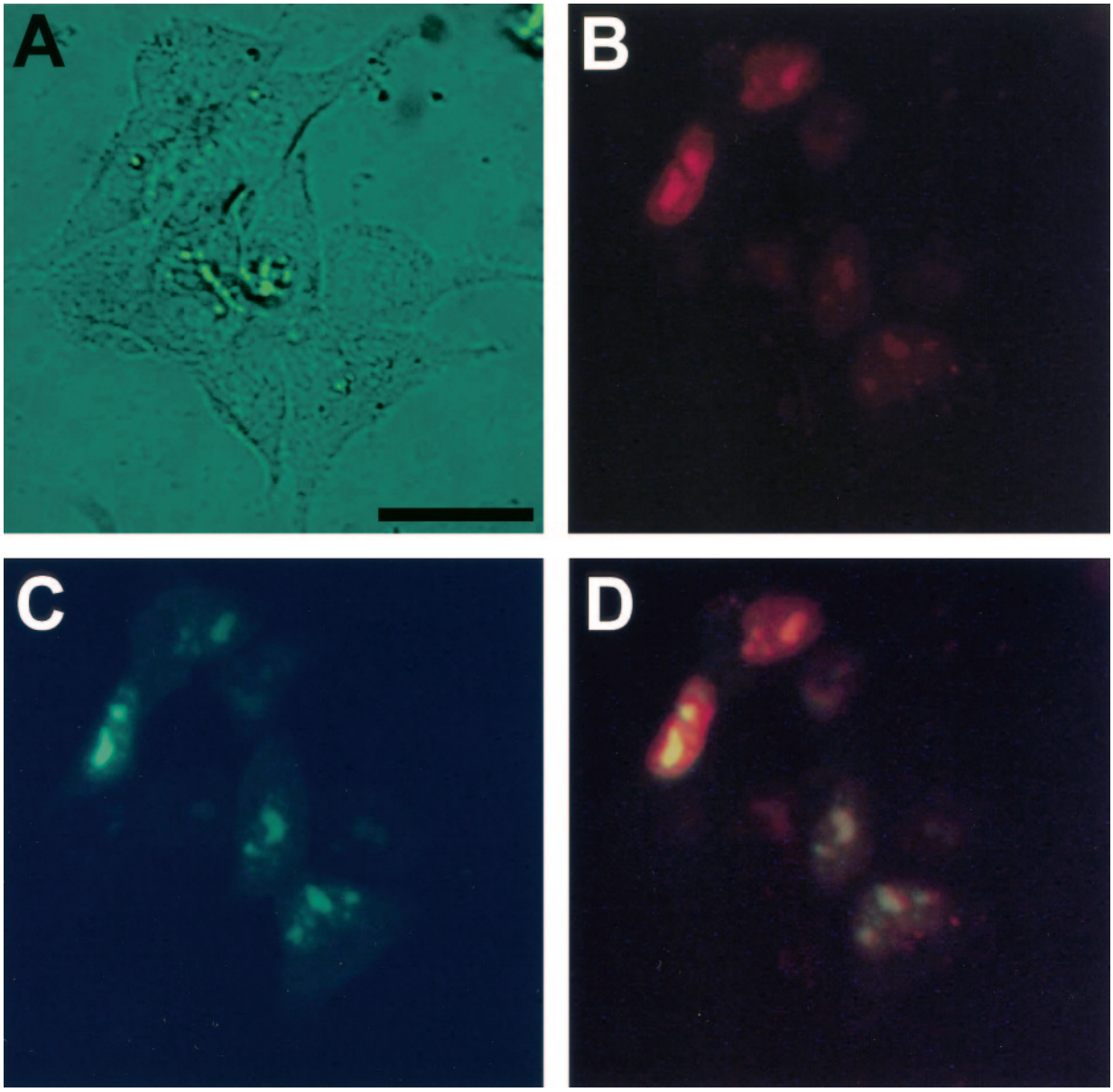

FIG. 5. Ectopic coexpression of mRFP-HANP1/H1T2 and EGFP-protamine fusion proteins in transfected cultured cells. HEK-293 cells were cotransfected with the expression vectors pmRFP-*Hanp1*/*H1T2* and pEGFP-Prm using Lipofectamine Plus reagent. The cells were observed 24 h after transfection using a Leica inverted fluorescence microscope under normal light (A) and with Leica fluorescein isothiocyanate filter sets for observation of the expression of mRFP (B) and GFP (C). (D) Merged image of mRFP and GFP fluorescence. Bar = 50 μm.

tamine antibody could be used for coprecipitation experiments. The coprecipitation of extracts of HEK 293 cells expressing both mRFP-HANP1/H1T2 and EGFP-protamine recombinant proteins indicated that HANP1/H1T2 associates with protamine either directly or indirectly (Fig. 4D). mRFP-HANP1/H1T2 did not associate with EGFP-*hils1* or histone H1, and mRFP-*hils1* did not associate with EGFP-protamine as a control (Fig. 4D). Figure 5 also shows that the recombinant EGFP–protamine-1 and mRFP-HANP1/H1T2 proteins were colocalized in the nuclei of HEK 293 cells and that these proteins were restricted to subnuclear foci within the nucleus. These results indicate that HANP1/H1T2 is able to associate with protamines.

Male *Hanp1*/*H1T2* null mice are infertile. To investigate the physiological role of HANP1/H1T2, we generated homozygous *Hanp1*/*H1T2* knockout mice. Homologous recombination was used to generate embryonic stem cell clones that were heterozygous for the *Hanp1*/*H1T2* mutation. To produce chimeric mice, the transgenic ES cells were injected into blastocysts that were subsequently implanted into pseudopregnant mice. The strategies used to produce the *Hanp1*/*H1T2* knockout mice and the Southern blot analysis of the mutant mice are shown in Fig. 6A and B. Crosses of heterozygous mutant pairs produced the expected ratio of wild-type, heterozygous, and homozygous genotype offspring, according to the classical Mendelian inheritance pattern. The body weights, growth rates of newborn

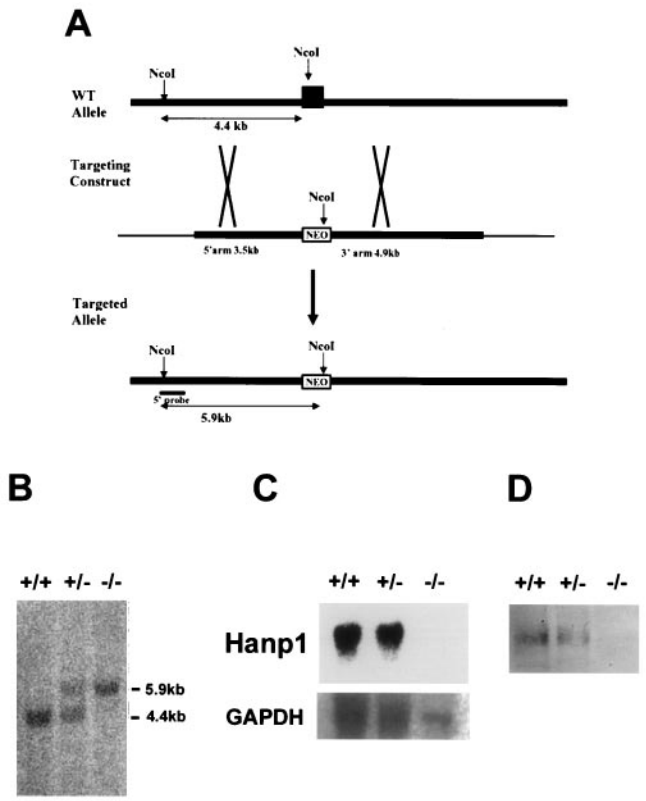

FIG. 6. *Hanp1/H1T2* gene targeting, identification, and expression of *Hanp1/H1T2* in gene-targeted mice. (A) Schematic representation of the strategy used for targeting the *Hanp1/H1T2* gene. The black box indicates the intronless *Hanp1/H1T2* gene. NcoI indicates the restriction enzyme recognition site. The gene targeting construct contained the neo gene (NEO in open box) placed between the 3.5-kb 5′ and the 4.9-kb 3′ homology arms. The thick and thin lines indicate the genomic and targeting vector DNA, respectively. (B) The targeted allele was identified by Southern blot analysis of NcoI-digested genomic DNA using a probe derived from the 5′ fragment of the vector. (C) Northern blot analysis. Transcripts of the *Hanp1/H1T2* gene were not detectable in the testes of homozygous *Hanp1/H1T2* knockout mice. The same filter was then rehybridized with a GAPDH cDNA probe as a control. (D) Western blot analysis of testicular lysates from adult mice using anti-HANP1/H1T2 antiserum. The HANP1/H1T2 protein was not detected in the testicular lysate of the homozygous *Hanp1/H1T2* knockout mouse. WT, wild type.

pups, and weights of various organs, including the testes and seminal vesicles of adult *Hanp1/H1T2* mutant mice, were not significantly different from those of wild-type mice. *Hanp1/H1T2* mRNA was not detectable by Northern blot analysis (Fig. 6C), and the 44-kDa HANP1/H1T2 protein was not detected on Western blots (Fig. 6D) of the testes of homozygous *Hanp1/H1T2* knockout mice. Microscopic examination of the testes did not show any significant differences among homozygous, heterozygous, and wild-type mice, but only homozygous *Hanp1/H1T2* male mutants were infertile. Matings between homozygous *Hanp1/H1T2* knockout males and wild-type females did not produce any successful pregnancies during more than 3 months of continuous cohabitation, even though many vaginal plugs were observed in the paired wild-type females (Table 1). The heterozygous male *Hanp1/H1T2* mutant mice and the homozygous females were all fertile and produced as many progeny per pregnancy as did their wild-type littermates.

TABLE 1. Fertility rate of mutant mice

Genotype	Male fertility[a]	Litter size[b]	Female fertility[c]	Litter size
+/+	10/10	8.1	10/10	8.4
+/−	10/10	8.6	10/10	9.0
−/−	0/10	0	10/10	8.4

[a] Number of fertile females per number of vaginal plugs.
[b] Average number of newborn pups.
[c] Wild-type males were mated with females of each genotype.

TABLE 2. Motility characteristics and in vitro fertilization of sperm from Hanp1-deficient mice

Genotype	*n*	Sperm no. (10^6)[a]	Motility (%)[b]	VCL	IVF
+/−	3	87 ± 7.5	93.0 ± 3.5	247.2 ± 10.3	98.8 ± 16.0
−/−	3	69 ± 16.0	23.7 ± 17.9*	148.8 ± 52.4*	0.0

[a] Number of sperm recovered from a cauda epididymis
[b] Motility (%) and curvilinear velocity (VCL) were measured after 1 h of incubation by computer-assisted sperm analysis. *, Statistically significant difference ($P < 0.01$).

***Hanp1/H1T2* knockout mice have defects in sperm nuclear formation.** Although similar numbers of sperm were recovered from the cauda epididymides of homozygous and heterozygous *Hanp1/H1T2* mutant males (Table 2), light microscopy showed that most of the sperm from homozygous *Hanp1/H1T2* mutants had abnormal kinks in the tails and abnormally shaped heads (Fig. 7a). Electron microscopy demonstrated that the step 6 spermatids from homozygous *Hanp1/H1T2* mutants exhibited nuclear abnormalities (Fig. 7b); the nuclear membranes were undulated, and the nuclei were invaginated. A clear halo was observed inside the nuclear membrane in mature spermatids (Fig. 7c) and epididymal sperm (Fig. 7d), apparently attributable to the condensed chromatin leaving an almost electron-transparent space near the nuclear membrane. These nuclear abnormalities were observed in cells at a stage of development in which HANP1/H1T2 expression normally occurs. Other observed abnormalities included dislocated necks of epididymal sperm (Fig. 7d); abnormalities in the heads of mature spermatids and sperm, such as remnants of the cytoplasm around the nucleus; and deformation and some vacuolation of the acrosomes (Fig. 7d). These abnormalities were found in germ cells that had differentiated beyond step 5, and no morphological abnormalities were found in earlier steps of spermiogenesis. Taken together, these findings indicate that the absence of HANP1/H1T2 expression leads to abnormalities in the formation of the spermatid nucleus, which in turn results in abnormal morphogenesis of other parts of the sperm, including the formation of kinks in the tails (14). Alternatively, the HANP1/H1T2 protein may directly affect various aspects of sperm morphogenesis.

***Hanp1/H1T2* mutant sperm exhibit abnormal movement.** As the morphological abnormalities described above appeared likely to cause motility defects in the mutant sperm, we performed computer-assisted sperm analysis to quantify the sperm motility after 1, 3, and 6 h of incubation in TYH medium (28). Table 2 shows the percent motility and the curvilinear velocity

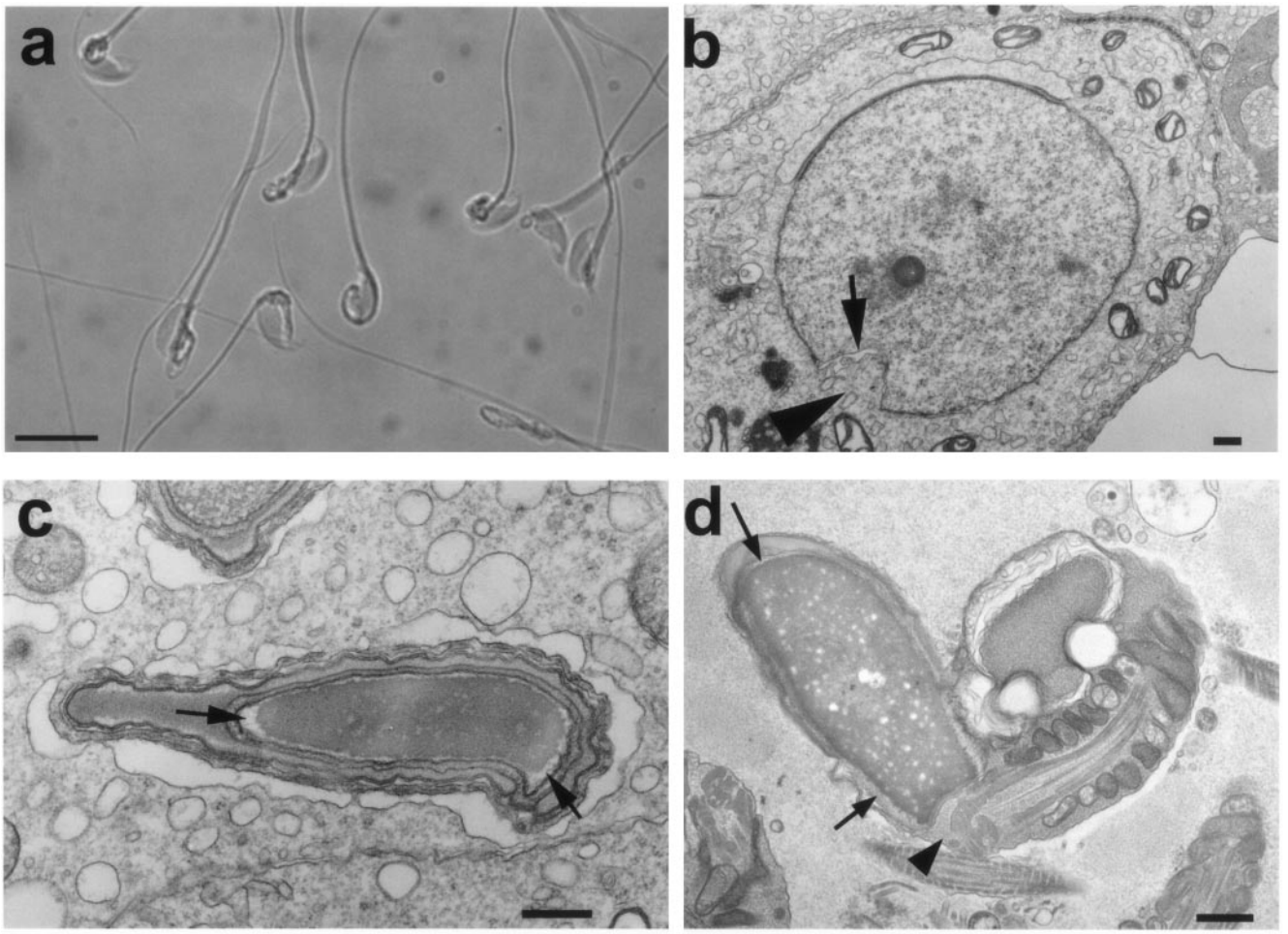

FIG. 7. Morphology of spermatids and sperm from homozygous *Hanp1/H1T2* mutant mice. (a) Light micrograph of cauda epididymal sperm. The mutant sperm have abnormal connections between the head and the neck. Bar = 10 μm. (b) Electron micrograph of a step 6 spermatid. The nuclear membrane is ruffled (arrow), and invagination of the nucleus is visible (arrowhead). Bar = 0.5 μm. (c) A step 12 spermatid. A pale halo can be observed under the nuclear membrane (arrows). Bar = 0.5 μm. (d) Sperm in the cauda epididymis. The arrows indicate a clear halo under the nuclear membrane. The sperm neck appears dislocated from the base of the head (arrowhead). Bar = 0.5 μm.

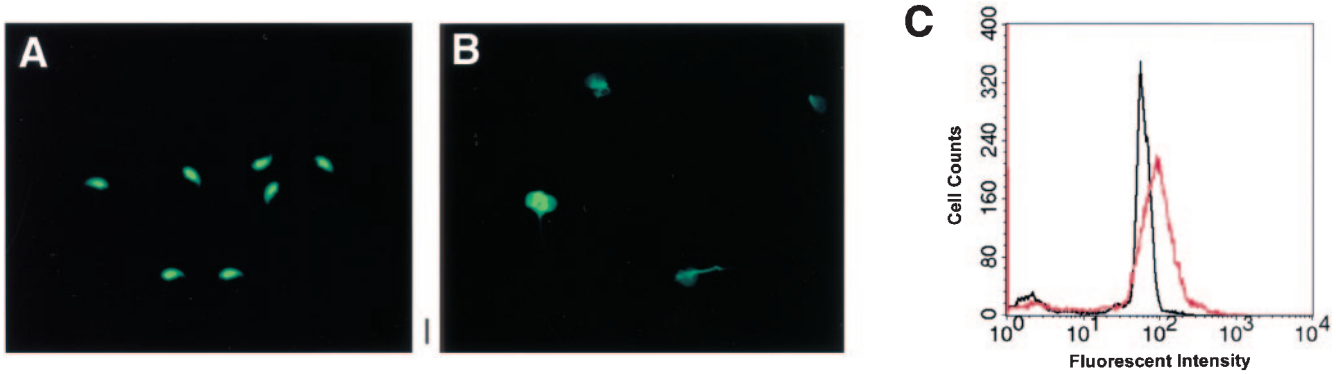

FIG. 8. Analysis of sperm from *Hanp1/H1T2* mutant mice. Sperm from heterozygous (A) and homozygous (B) *Hanp1/H1T2* mutant mice were stained with acridine orange (AO) and observed under UV light after being incubated in a medium containing 0.5 M β-mercaptoethanol. The nuclei of all sperm from homozygous mutant mice were disrupted by exposure to reducing conditions. Bar = 10 μm. (C) FACS analysis of sperm stained with propidium iodide (PI). Red and black indicate homozygous and heterozygous *Hanp1/H1T2* mutant sperm, respectively. Sperm from homozygous mice were stained more strongly and less homogeneously with PI than were control sperm.

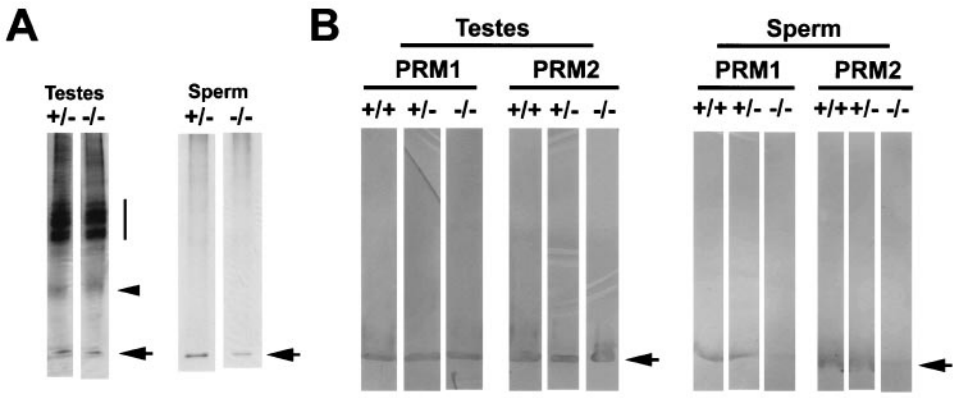

FIG. 9. Expression of protamine-1 and -2 in testes and sperm of *Hanp1*/*H1T2* mutant mice. Tissue lysates were electrophoresed in an acid-urea gel, and the proteins were stained with Coomassie brilliant blue (A) or subjected to Western blot analysis using anti-protamine monoclonal antibodies (B). Similar amounts of both protamine-1 and -2 (PRM1 and PRM2) were expressed in the testes of wild-type mice and of both homozygous and heterozygous *Hanp1*/*H1T2* mutant mice. In contrast, both protamines were only weakly detected in sperm from homozygous *Hanp1*/*H1T2* mutant mice (A). The arrows indicate the position of the protamine bands. The bar and arrowhead in panel A indicate the positions of histones and transition proteins, respectively.

observed after 1 h of incubation. The sperm from homozygous *Hanp1*/*H1T2* null mutant mice exhibited decreases in the ratio of motile sperm, the measurable velocities (including average path velocity, straight line velocity, and curvilinear velocity), and the amplitude of the lateral head displacement after 1 to 6 h of incubation compared with sperm from normal mice (data not shown). These observations indicated that the observed morphological abnormalities of the sperm from *Hanp1*/*H1T2* knockout mice may impair sperm movements and that the viability and maturation of the sperm are otherwise normal in these animals. The mutant sperm were insufficiently motile to fertilize eggs by in vitro fertilization (Table 2), although they could successfully bind to the zona pellucida in vitro. In contrast, *Hanp1*/*H1T2* mutant sperm could support fertilization and embryo development after ICSI. Sperm derived from two heterozygous and two homozygous *Hanp1*/*H1T2* mutant mice were injected into 92 and 106 eggs, respectively, from which 21 (27%) and 23 (28%) pups were born, respectively.

DNA is loosely packaged in *Hanp1*/*H1T2* null sperm. During normal chromatin remodeling in sperm, histones are replaced by protamines. Protamines form disulfide bond bridges, contributing to the chromatin in sperm nuclei being more densely packed than the chromatin in somatic cells. To examine the integrity of chromatin packaging in the homozygous *Hanp1*/*H1T2* mutant sperm, the reducing agent β-mercaptoethanol was added to sperm suspended in TYH medium. Although both wild-type and heterozygous *Hanp1*/*H1T2* mutant sperm tolerated the resulting reducing conditions without changes in nuclear morphology, all of the nuclei of the homozygous mutant sperm lost integrity (Fig. 8A and B). The chromatin packaging in the mutant sperm was also examined by staining the nuclear DNA with the intercalating dye propidium iodide and analyzing the cells by FACS (33). A substantial number of the sperm from homozygous *Hanp1*/*H1T2* mutants exhibited stronger staining and yielded a higher fluorescence peak than did the control sperm (Fig. 8C), indicating that propidium iodide had greater access to the nuclear DNA in the mutant sperm than in the wild-type sperm. Together, these observations suggested that the nuclei of sperm from *Hanp1*/*H1T2* mutant mice are easily disrupted and that the condensation of the nuclear DNA in *Hanp1*/*H1T2* mutant sperm is incomplete.

Protamine content is decreased in *Hanp1*/*H1T2* null sperm. Protamines are important molecules in the packaging of genomic DNA and the formation of the final chromatin pattern in sperm (5). Although normal levels of protamine-1 and -2 were detected in the testes of homozygous *Hanp1*/*H1T2* mutant mice, the levels detected in epididymal sperm were lower than those in controls (Fig. 9A). Western blotting with anti-protamine antibodies confirmed that the levels of both protamines in homozygous *Hanp1*/*H1T2* mutant sperm were quantitatively and/or qualitatively reduced (Fig. 9B) compared with the levels in sperm from wild-type mice. In contrast, there were no significant differences in the intensity of the protamine signal between the sperm from heterozygous and homozygous mice (Fig. 9A and 10). Furthermore, higher magnification images showed that both protamine-1 and -2 were highly restricted to the cell nuclei of elongated spermatids from heterozygous (Fig. 10) and wild-type mice (data not shown). In contrast, in elongated spermatids from homozygous *Hanp1*/*H1T2* mutant mice, protamine-1 was unevenly localized to the nuclei and aggregated around the nuclear region, and protamine-2 was distributed diffusely in the cytoplasm around the nuclei. Immunohistochemical observation of sperm with anti-protamine antibodies also showed minimal staining of the homozygous mutant sperm (Fig. 10B).

These results indicated that HANP1/H1T2 is necessary for the precise localization of protamines to the nuclei of elongated spermatids and spermatozoa and that the mutation of *Hanp1*/*H1T2* causes a substantial reduction in the protamine levels in the sperm or that protamines are not folded in the sperm nucleus in the same manner as in the wild-type but not in the testis.

DISCUSSION

Dramatic remodeling of chromatin takes place during mammalian spermiogenesis. Nuclear elongation and chromatin condensation occur concomitantly with modifications in the basic nuclear proteins associated with DNA. A number of

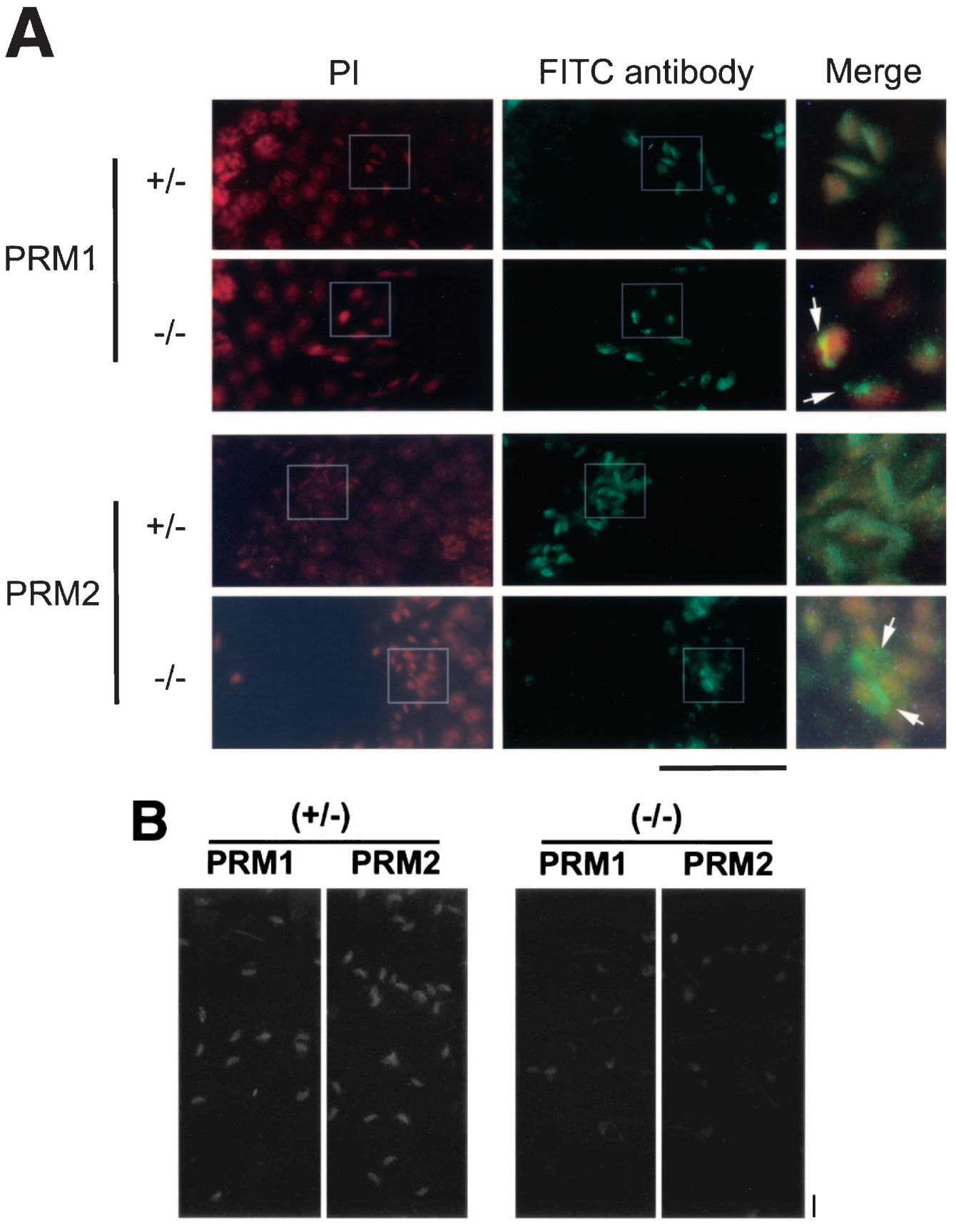
A
PI
FITC antibody
Merge
PRM1
+/-
-/-
PRM2
+/-
-/-
B
(+/-)
(-/-)
PRM1
PRM2
PRM1
PRM2

biochemical events accompany the displacement of histones and the appearance of a set of basic nuclear proteins such as tH2A, tH2B, H1t, spermatid-specific H2B (ssH2B), testis-specific HMG (tsHMG), histone H1-like protein in spermatids 1 (Hils 1), transition proteins (TNPs), and protamines (2, 3, 12, 13, 17, 20, 31). Histone synthesis ceases during spermiogenesis, and histones are replaced by a set of TNPs, which are subsequently replaced by protamines (2, 20). The completed process results in greater condensation of mitotic chromosomes, producing a tightly packaged chromatin structure. Recently, it was reported that some testicular nuclear proteins, such as protamines in sperm, have probably evolved from a primordial histone H1 (18). The chromatin structure of haploid germ cells has been complicated by the evolutionary replication of linker histone H1. Strong expression of linker histone H1 variants is important for the formation of sperm nuclei (21).

In this study, we identified a novel histone H1-like haploid germ-cell-specific nuclear protein designated HANP1/H1T2 that has an RS domain. HANP1/H1T2 is specifically expressed during chromatin remodeling and is mainly localized to the nucleus during spermiogenesis. Although homology of the complete amino acid sequence of HANP1/H1T2 with the histone H1 sequences of other organisms is not high (1), the homology with the globular H1 domain is substantial (35%). The HANP1/H1T2 protein in the mouse and its human homolog may also be evolutionarily derived from histone H1.

The finding that a portion of the endogenous HANP1/H1T2 in nuclear lysates of testicular germ cells was able to bind to DNA and that a substantial amount of HANP1/H1T2 was nonetheless recovered in the flowthrough fraction from DNA-cellulose columns indicated that HANP1/H1T2 protein, or its complexes, has two different forms with different DNA-binding abilities. HANP1/H1T2 protein also has an ATP-binding domain (23) and binds to ATP-cellulose columns. It has been reported that the functions of histones and other nuclear proteins are regulated by ATP and by phosphorylation (4, 8). Our findings therefore suggest that the DNA-binding ability of HANP1/H1T2 may be regulated by the binding of ATP to the ATP-binding domain. We attempted to examine the biochemistry of HANP1/H1T2 in more detail by purifying recombinant HANP1/H1T2 from *Escherichia coli* transformed with an expression vector. However, the transformed *E. coli* cells died rapidly, although expression of the recombinant protein was not induced. This observation suggests that a low level of "leaky" HANP1/H1T2 expression in *E. coli* was sufficient to induce cell death.

To investigate the physiological role of HANP1/H1T2 in chromatin condensation during spermiogenesis, we generated *Hanp1/H1T2* null mutant mice. The homozygous *Hanp1/H1T2* knockout mice exhibited aberrant chromatin packaging in the sperm nucleus and abnormal nuclear formation (14). Recent studies have suggested that the docking of protamine-1 to the nuclear envelope is an important intermediate step in spermiogenesis and have revealed novel roles for SR protein kinases and p32 (22). The observations that HANP1/H1T2 and protamines are expressed during similar steps of spermatid differentiation and that these proteins can be coimmunoprecipitated suggest that the recruitment of protamines into chromatin may be regulated by HANP1/H1T2, which has an RS domain. The HANP1/H1T2 protein colocalized with protamines in spermatid nuclei and associated with protamines in a direct or indirect manner, as supported by coimmunoprecipitation experiments using cotransfected HEK 293 cells in which no other spermatid-specific proteins were present. The observed abnormalities in the formation of spermatid nuclei in *Hanp1/H1T2* knockout mice indicated that HANP1/H1T2 might also be involved in chromatin formation during spermiogenesis.

Recent studies have shown that the inactivation of even one genome copy of either the protamine-1 or -2 gene resulted in the production of abnormal sperm and caused male infertility attributable to haploinsufficiency (5). Protamine-2 gene-deficient sperm, produced in chimeric mice resulting from injection of protamine-2 gene-deficient ES cells into wild-type blastocysts, were unable to induce embryonic development even by ICSI (6). Thus, the inability of sperm with reduced amounts of protamine-2 to successfully fertilize eggs or to induce embryogenesis is probably attributable to the loss of proper packaging of chromosomal DNA in the sperm, which, in turn, leaves the DNA susceptible to both damage and strand repair failure (6). In contrast, when homozygous *Hanp1/H1T2* mutant sperm were subjected to ICSI in this study, we obtained fairly efficient fertilization, normal embryogenesis, and healthy pups. Thus, it appears that the loss of protamines from sperm does not necessarily result in the deterioration of normal functioning of the sperm nuclei during fertilization, although sufficient protamine levels are important for proper chromatin and nuclear formation in spermatozoa. Alternatively, protamines may be important in spermiogenesis but not in the formation of the sperm head, such that a trace of protamine in the *Hanp1/H1T2* knockout sperm would be sufficient to support fertilization and development of embryos by ICSI, even though the packaging of the chromatin in the sperm was abnormal.

TNP1 and TNP2 are found in rodent spermatids, are be-

FIG. 10. Immunostaining of protamine-1 and -2 in the testes of heterozygous and homozygous *Hanp1/H1T2* mutant mice. PRM1 and PRM2 indicate immunofluorescent staining using anti-protamine-1 and -2 monoclonal antibodies, respectively. (A) Sections of testes. PI indicates nuclei stained with propidium iodide. The fluorescence signals of the secondary fluorescein isothiocyanate (FITC)-labeled anti-mouse antibody indicate that the localization of protamine-1 or -2 was limited to haploid spermatids during the later stages of differentiation (elongated spermatids). The area indicated by the white boxes was enlarged and merged. The signals of both protamine-1 and -2 were distributed in the nuclei of the control heterozygous mutant, whereas no nuclear-specific staining was observed in the homozygous *Hanp1/H1T2* mutant mice. The staining patterns of protamine-1 and -2 differed in the mutants (white arrows); the former appeared as dot-like aggregates in and around the nuclei, and the latter appeared as a diffuse staining in the cytoplasm around the nuclei. Bar = 50 μm. (B) Positively stained signals of both protamines were barely detectable in *hanp1* homozygous mutant sperm. Bar = 10 μm.

lieved to be the predominant transition proteins for chromatin remodeling in mammalian spermiogenesis, and are thought to be involved in histone displacement and chromatin condensation. Male mice with null mutations in either TNP1 or TNP2 were fertile, although their fertility was reported to be reduced (32, 33). However, mice in which both TNP genes were disrupted were completely sterile (34). The sperm produced by mice lacking both TNP1 and TNP2 contained immature protamines in the nuclei; the nuclei remained immature, the chromatin was incompletely packed by protamines, and the sperm nuclei were rapidly disrupted by exposure to reducing conditions (34). Although the double-mutant nuclei could successfully support embryogenesis after ooplasmic round spermatid-nuclear injection, no pups were produced by ICSI (34). This differs from our ICSI results using sperm from homozygous *Hanp1*/*H1T2* knockout mice. Together, these results indicate that the nuclei of sperm from mice with both TNPs disrupted are more unstable than those of sperm from homozygous *Hanp1*/*H1T2* knockout mice. The abnormal distribution of protamine-1 and -2 in some elongated spermatids in the testes of homozygous *Hanp1*/*H1T2* knockout mice suggests that HANP1/H1T2 is involved in chromatin remodeling, together with TNPs. Thus, to further the understanding of the role of HANP1/H1T2 in chromatin remodeling, it will be necessary to investigate the associations between HANP1/H1T2 and other nuclear proteins, as well as those between TNPs and protamines.

Our results indicate that HANP1/H1T2 is a novel protein essential for the packaging of protamine and DNA into chromatin in sperm and for the formation of the compact sperm nucleus that is required for natural fertilization. However, these conditions are not necessarily prerequisites for the production of healthy pups if the initial process of fertilization is bypassed by assisted microfertilization. We suggest that mutations or disruptions of the *Hanp1*/*H1T2* gene may underlie some cases of human infertility. In addition, future research on the biochemical characteristics of HANP1/H1T2 may contribute to an understanding of the formation of the nucleus during spermiogenesis.

ACKNOWLEDGMENTS

We acknowledge IngenKO Pty. Ltd., Australia, for their help in producing the *Hanp1*/*H1T2* mutant mice. We thank Balhorn Rod for providing the monoclonal antibodies to protamine-1 and -2. We also thank Hiromi Nishimura, Kahori Numazawa, and Amy Herlihy for their technical assistance, and Textcheck and Stephanie L. Cook for editing the manuscript.

REFERENCES

1. **Ali, T., P. Coles, T. J. Stevens, K. Stott, and J. O. Thomas.** 2004. Two homologous domains of similar structure but different stability in the yeast linker histone, Hho1p. J. Mol. Biol. **338:**139–148.
2. **Balhorn, R.** 1982. A model for the structure of chromatin in mammalian sperm. J. Cell Biol. **93:**298–305.
3. **Boissonneault, G., and Y. F. Lau.** 1993. A testis-specific gene encoding a nuclear high-mobility-group box protein located in elongating spermatids. Mol. Cell. Biol. **13:**4323–4330.
4. **Cheung, P., C. D. Allis, and P. Sassone-Corsi.** 2000. Signaling to chromatin through histone modifications. Cell **103:**263–271.
5. **Cho, C., W. D. Willis, E. H. Goulding, H. Jung-Ha, Y. C. Choi, N. B. Hecht, and E. M. Eddy.** 2001. Haploinsufficiency of protamine-1 or -2 causes infertility in mice. Nat. Genet. **28:**82–86.
6. **Cho, C., H. Jung-Ha, W. D. Willis, E. H. Goulding, P. Stein, Z. Xu, R. M. Schultz, N. B. Hecht, and E. M. Eddy.** 2003. Protamine 2 deficiency leads to sperm DNA damage and embryo death in mice. Biol. Reprod. **69:**211–217.
7. **de Rooij, D. G., M. Okabe, and Y. Nishimune.** 1999. Arrest of spermatogonial differentiation in jsd/jsd, Sl17H/Sl17H, and cryptorchid mice. Biol. Reprod. **61:**842–847.
8. **Dou, Y., and M. A. Gorovsky.** 2000. Phosphorylation of linker histone H1 regulates gene expression *in vivo* by creating a charge patch. Mol. Cell **6:**225–231.
9. **Fujii, T., K. Tamura, K. Masai, H. Tanaka, Y. Nishimune, and H. Nojima.** 2002. Use of stepwise subtraction to comprehensively isolate mouse genes whose transcription is up-regulated during spermiogenesis. EMBO Rep. **3:**367–372.
10. **Graveley, B. R.** 2004. A protein interaction domain contacts RNA in the prespliceosome. Mol. Cell **13:**302–304.
11. **Ho, Y., K. Wigglesworth, J. J. Eppig, and R. M. Schultz.** 1995. Preimplantation development of mouse embryos in KSOM: augmentation by amino acids and analysis of gene. Mol. Reprod. Dev. **41:**232–238.
12. **Huh, N. E., I. W. Hwang, K. Lim, K. H. You, and C. B. Chae.** 1991. Presence of a bi-directional S phase-specific transcription regulatory element in the promoter shared by testis-specific TH2A and TH2B histone genes. Nucleic Acids Res. **19:**93–98.
13. **Iguchi, N., H. Tanaka, K. Yomogida, and Y. Nishimune.** 2003. Isolation and characterization of a novel cDNA encoding a DNA-binding protein (Hils1) specifically expressed in testicular haploid germ cells. Int. J. Androl. **26:**354–365.
14. **Kimura, T., C. Ito, S. Watanabe, T. Takahashi, M. Ikawa, K. Yomogida, Y. Fujita, M. Ikeuchi, N. Asada, K. Matsumiya, A. Okuyama, M. Okabe, K. Toshimori, and T. Nakano.** 2003. Mouse germ cell-less as an essential component for nuclear integrity. Mol. Cell. Biol. **23:**1304–1315.
15. **Kimura, Y., and R. Yanagimachi.** 1995. Intracytoplasmic sperm injection in the mouse. Biol. Reprod. **52:**709–720.
16. **Koga, M., H. Tanaka, K. Yomogida, M. Nozaki, J. Tsuchida, H. Ohta, Y. Nakamura, K. Masai, Y. Yoshimura, M. Yamanaka, N. Iguchi, H. Nojima, K. Matsumiya, A. Okuyama, and Y. Nishimune.** 2000. Isolation and characterization of a haploid germ cell-specific novel complementary deoxyribonucleic acid; testis-specific homologue of succinyl CoA:3-Oxo acid CoA transferase. Biol. Reprod. **63:**1601–1609.
17. **Kremer, E. J., and W. S. Kistler.** 1991. Localization of mRNA for testis-specific histone H1t by *in situ* hybridization. Exp. Cell Res. **197:**330–332.
18. **Lewis, J. D., N. Saperas, Y. Song, M. J. Zamora, M. Chiva, and J. Ausio.** 2004. Histone H1 and the origin of protamines. Proc. Natl. Acad. Sci. USA **101:**4148–4152.
19. **Li, E.** 2002. Chromatin modification and epigenetic reprogramming in mammalian development. Nat. Rev. Genet. **3:**662–673.
20. **Mali, P., A. Kaipia, K. Kangasniemi, J. Toppari, M. Sandberg, N. B. Hecht, and M. Parvinen.** 1989. Stage-specific expression of nucleoprotein mRNAs during rat and mouse spermiogenesis. Reprod. Fertil. Dev. **1:**369–382.
21. **Martianov, I., S. Brancorsini, R. Catena, A. Gansmuller, N. Kotaja, M. Parvinen, P. Sassone-Corsi, and I. Davidson.** 2005. Polar nuclear localization of H1T2, a histone H1 variant, required for spermatid elongation and DNA condensation during spermiogenesis. Proc. Natl. Acad. Sci. USA **102**: 2808–2813.
22. **Mylonis, I., V. Drosou, S. Brancorsini, E. Nikolakaki, P. Sassone-Corsi, and T. Giannakouros.** 2004. Temporal association of protamine 1 with the inner nuclear membrane protein lamin B receptor during spermiogenesis. J. Biol. Chem. **279:**11626–11631.
23. **Neuwald, A. F., L. Aravind, J. L. Spouge, and F. Koonin.** 1999. AAA+: a class of chaperone-like ATPases associated with the assembly, operation, and disassembly of protein complexes. Genome Res. **9:**27–43.
24. **Russell, L. D., R. A. Ettlin, H. A. P. Sinha, and E. D. Clegg.** 1990. Mammalian spermatogenesis, p. 1–40. *In* L. D. Russell, R. A. Ettlin, H. A. P. Sinha, and E. D. Clegg (ed.), Histological and histopathological evaluation of the testis. Cache River Press, St. Louis, Mo.
25. **Sassone-Corsi, P.** 2002. Unique chromatin remodeling and transcriptional regulation in spermatogenesis. Science **296:**2176–2178.
26. **Stanker, L. H., A. Wyrobek, and R. Balhorn.** 1987. Monoclonal antibodies to human protamines. Hybridoma **6:**293–303.
27. **Tanaka, H., L. A. Pereira, M. Nozaki, J. Tsuchida, K. Sawada, H. Mori, and Y. Nishimune.** 1997. A germ cell-specific nuclear antigen recognized by a monoclonal antibody raised against mouse testicular germ cells. Int. J. Androl. **20:**361–366.
28. **Tanaka, H., N. Iguchi, Y. Toyama, K. Kitamura, T. Takahashi, K. Kaseda, M. Maekawa, and Y. Nishimune.** 2004. Mice deficient for the axonemal protein tektin-t exhibit male infertility and immotile cilia syndrome due to impaired inner arm dynein function. Mol. Cell. Biol. **24:**7956–7964.
29. **Tanaka, H., and T. Baba.** 2005. Gene expression in spermiogenesis. Cell. Mol. Life Sci. **62:**344–354.
30. **Toyoda, Y., M. Yokoyama, and T. Hoshi.** 1971. Studies on the fertilization of mouse egg *in vitro*. Jpn. J. Anim. Reprod. **16:**147–151.
31. **Yan, W., L. Ma, K. H. Burns, and M. M. Matzuk.** 2003. HILS1 is a sper-

matid-specific linker histone H1-like protein implicated in chromatin remodeling during mammalian spermiogenesis. Proc. Natl. Acad. Sci. USA **100:** 10546–10551.

32. **Yu, Y. E., Y. Zhang, E. Unni, C. R. Shirley, J. M. Deng, L. D. Russell, M. M. Weil, R. R. Behringer, and M. L. Meistrich.** 2000. Abnormal spermatogenesis and reduced fertility in transition nuclear protein 1-deficient mice. Proc. Natl. Acad. Sci. USA **97:**4683–4688.
33. **Zhao, M., C. R. Shirley, Y. E. Yu, B. Mohapatra, Y. Zhang, E. Unni, J. M. Deng, N. A. Arango, N. H. Terry, M. M. Weil, L. D. Russell, R. R. Behringer, and M. L. Meistrich.** 2001. Targeted disruption of the transition protein 2 gene affects sperm chromatin structure and reduces fertility in mice. Mol. Cell. Biol. **21:**7243–7255.
34. **Zhao, M., C. R. Shirley, S. Hayashi, L. Marcon, B. Mohapatra, R. Suganuma, R. R. Behringer, G. Boissonneault, R. Yanagimachi, and M. L. Meistrich.** 2004. Transition nuclear proteins are required for normal chromatin condensation and functional sperm development. Genesis **38:**200–213.